Ragul S[1],
Raghavendran P S[2],
Ramesh S[3]

Optimization of Bidirectional Converters and BLDC Motor Control in Microgrids Using Priority Adaptive Particle Optimization Driven Boosting Model

Journal of Electrical Systems

Abstract

With renewable energy sources integrated seamlessly into modern power grids, the control strategies should be proficient to optimize energy flow and ensure system stability. Thus, grid-connected microgrids play an important role in this transition by balancing generation and consumption using sophisticated optimization techniques. This paper presents a Priority Adaptive Particle Optimization (PAPO) framework with Gradient Boosting Decision Trees (GBDT) to efficiently control bidirectional power converters in microgrids. The PAPO algorithm dynamically adjusts the real-time control parameters to optimize the efficiency of Brushless DC (BLDC) motors in response to variations in loads and environmental conditions. Furthermore, high-gain converters are used for better integration of RESs such as solar and wind with less switching losses and improved energy conversion efficiency. Energy management, considering the synergy of PAPO-GBDT, accurately models both demand on the load side and generation on the supply side. The proposed framework was implemented in MATLAB/Simulink using conventional optimization techniques for validation. The results presented better performance in terms of minimized power losses, energy efficiency, and stable operation of the microgrid. The PAPO-GBDT framework showed a 15% decrease in energy losses and a 10% improvement in overall energy conversion efficiency compared to traditional optimization methods. The system also ensured stable microgrid operation with a 98% reliability rate under changing environmental conditions.

Keywords: Adaptive Optimization, Gradient Boosting, Microgrids, Renewable Energy, Bidirectional Power Converters and Energy Flow.

1. INTRODUCTION

The rapid adoption of renewable energy sources, such as solar and wind energy, has made a significant contribution to the transition of the global landscape in terms of energy [1]. Currently, grid-connected microgrids are considered significant components of power systems. They provide localized energy solutions by integrating different types of distributed energy resources, along with storage systems and controllable loads, all while ensuring effective energy flow from the microgrid to the primary grid [2]. However, the effective use of microgrids needs advanced optimization strategies to overcome the challenges related to bidirectional power conversion, energy management, and system stability. In microgrid systems, the bidirectional converters play a very important role in regulating the flow of energy between the grid, renewable energy sources, and storage systems. The converters must ensure high efficiency, minimal switching losses, and seamless power transfer under dynamic operating conditions [3]. BLDC motors are frequently used in energy applications and need to be controlled appropriately so that they are maximally efficient under various environmental and load conditions.

[1] *Assistant Professor,*
Department of Electrical and Electronics Engineering,
Kongunadu College of Engineering and Technology, Thottiyam,Trichy, India.
[2]*Associate Professor,*
Department of Electrical and Electronics Engineering,
Kongu Engineering College, Perundurai, Erode, India.
[3] *Professor,*
Department of Electrical and Electronics Engineering,
K.S.R College of Engineering, Namakkal, India.
[1] raguleee78@gmail.com, [2]raghavendran@kongu.ac.in, [3]rameshksrce@gmail.com

The conventional control methods fail to fulfill these requirements because they do not adapt themselves to the real-time variation, which results in suboptimal energy utilization and increased system loss.

To overcome these limitations, optimization techniques such as Priority Adaptive Particle Optimization (PAPO) and Gradient Boosting Decision Trees (GBDT) have emerged as promising solutions. PAPO is a robust metaheuristic algorithm designed to dynamically adapt control parameters in real-time, ensuring optimal system performance under varying conditions [4-6]. On the other hand, GBDT, a machine learning-based boosting model, has excellent performance in modeling complex relationships and predicting control strategies based on load-side demand and supply-side generation. The combination of PAPO and GBDT offers a powerful framework to optimize energy flow in microgrids by utilizing their complementary strengths. The Priority Adaptive Particle Optimization (PAPO) technique is specifically suited for solving the challenges associated with bidirectional converter control and BLDC motor efficiency. PAPO in real time, self-tunes key control parameters, such as switching frequency and duty cycle to minimize switching losses and optimize energy conversion efficiency. Real-time feedback in the system makes it self-adaptive under varying operating conditions; hence, there is a consistent output across different scenarios. PAPO's adaptive nature makes it quite appropriate for the optimization of BLDC motor operation, which in turn requires very controlled modes of operation to achieve high efficiency in microgrid applications [7,8].

To complement PAPO, Gradient Boosting Decision Trees (GBDT) provide a data-driven approach to model and predict optimal control strategies for microgrid systems. GBDT works much better with nonlinear relationships and patterns in datasets, and it is very useful in energy management. By incorporating GBDT with PAPO, the proposed framework allows for accurate prediction and real-time adaptation of control strategies to ensure optimal energy flow and stabilize the system. High-gain converters [9] are essential to integrating renewable energy sources into microgrids because they allow proper transfer and regulation of power; the PAPO-GBDT framework is proposed to improve the performance of converters under real-time feedback from the systems, therPAPOre reducing switching losses but also improving practical use for renewable energy sources. Ensuring efficient energy transfer between the microgrid and the main grid will also address the fundamental challenges of operating a microgrid, including issues of energy wastage, poor power quality, and system instability.

Renewable energy sources have some challenges that come with their intermittent nature and dependence on environmental conditions. For instance, solar and wind energy are very volatile and thus require advanced control strategies to ensure balance in the system. The PAPO-GBDT framework addresses such challenges by adapting control strategies based on real-time data of the system, thus ensuring efficient energy utilization and reducing the effects of variability in renewable energy sources on the performance of microgrids. The effectiveness of the proposed framework was validated through PAPO-GBDT methodology implementation on MATLAB/Simulink. Simulations proved ample energy efficiency, system stability, and proper utilization of renewable energy sources in a microgrid. The framework was also proved superior over conventional optimization methods in minimizing power losses and optimizing the flow of energy within a microgrid. This research contributes to the growing literature on microgrid optimization by coming up with an innovative adaptive control strategy that puts together PAPO and GBDT. A novel framework which deals with bidirectional converter control efficiency and BLDC motor efficiency is proposed; thus, it acts as a stepping stone toward the building of sustainable, intelligent energy systems. The PAPO-GBDT framework is a robust solution for optimizing microgrid operations in modern power systems by enhancing the practical utilization of renewable energy sources and improving system performance. The major contributions of the research is,

- This paper proposes a new hybrid optimization approach called PAPO with GBDT. This novel hybrid optimization algorithm is applied for optimizing energy flow and system stability in grid-connected microgrids. It also controls the bidirectional converters and BLDC motors much better.
- The proposed framework enhances the performance of bidirectional converters and BLDC motors. PAPO allows for optimizing the control parameters for the minimum switching loss and ensures maximum efficiency. GBDT predicts optimal control strategies from real-time system data. This leads to smoother power transfer and better utilization of renewable sources.
- The proposed framework was tested and validated using MATLAB/Simulink simulations. Results show improvements in energy efficiency, system stability, and the use of renewable energy. Compared to traditional

optimization techniques, the proposed method excelled. This shows that PAPO-GBDT has huge potential for use in future applications in microgrids.

The rest of this paper is organized as follows: Section 2 describes the related work and existing optimization techniques for microgrid systems. Section 3 outlines the proposed PAPO-GBDT methodology with the mathematical modeling and system architecture. Section 4 presents simulation results and performance evaluation of the proposed framework. Finally, Section 5 concludes the paper and gives some insights into future research directions.

2. LITERATURE REVIEW

This literature review aims to examine and synthesize the current advancements and methodologies in the field of motor control, especially within the context of Brushless DC (BLDC) motors and their integration into a variety of control systems.

The Perturb and Observe (P&O) algorithm [10] is one of the most widely used Maximum Power Point Tracking (MPPT) techniques in photovoltaic (PV) systems. It works by perturbing the operating point of the system and observing the resulting changes in power to determine the direction of the maximum power point. However, the classical P&O algorithm suffers from several drawbacks, especially under conditions of rapidly changing environmental conditions, such as partial shading and fast irradiance changes. The algorithm might oscillate around the MPP or fail to track it properly under such dynamic conditions, leading to performance losses in real-time applications.

Particle Swarm Optimization (PSO) is an optimization algorithm inspired by the social behavior of birds flocking or fish schooling [11]. In the context of MPPT, PSO is applied to optimize the tracking of the maximum power point in PV systems. It provides real-time optimization by adjusting the control parameters based on the state of the system. Although PSO has been effective in enhancing the accuracy of MPPT, it suffers from premature convergence, where the algorithm may get stuck in local optima, thus preventing global optimization. The performance of PSO will degrade in the highly dynamic and nonlinear behaviors. For this kind of behavior, much advanced tuning and hybridization of the techniques might be needed.

Grey Wolf Optimizer is one type of nature-inspired optimization algorithm simulating leadership hierarchy and hunting behavior of gray wolves. It was used as GWO for MPPT application in [12], where balance between exploration and exploitation has led to fast convergence to the point of maximum power. It has proven effective for MPPT in PV systems, wherein rapid adaptation to changes in environmental conditions is highly crucial. Nevertheless, GWO's performance degrades with a complex dynamic environment that is subject to many local optima or noisy signals. This raises a need for further improvement or hybrid approaches for the sake of high accuracy and efficiency under variable conditions of PV system operations.

The Artificial Bee Colony (ABC) algorithm is a nature-inspired optimization [13] technique that is based on the foraging behavior of honey bees. ABC has been appreciated in MPPT applications for its computational efficiency, especially for unimodal objective functions where the search space is simple. It can efficiently find optimal or near-optimal solutions with relatively low computational overhead. However, the ABC algorithm struggles in multi-modal functions with many peaks or local optima in the search space. It can get poor in high-dimensional search spaces, so some modification or hybridization is necessary to improve its robustness and efficiency in complex environments.

The Grasshopper Optimization Algorithm (GOA) simulates [14] grasshoppers' natural social behavior: the whole group moves toward the optimal solution together. GOA is a strong global explorer with fast convergence speed, and it is therPAPOre an effective optimization algorithm for MPPT in PV systems. The algorithm is well-suited to dynamic environments where fast tracking of maximum power is essential. However, GOA may require fine-tuning of its parameters to achieve optimal performance, particularly in scenarios with complex or changing input conditions. Despite the strengths, exploration vs exploitation balance can be difficult in certain high-dimension or noisy environments.

The paper presented here in [15] deals with neural network-based controller for a BLDC motor. Here the model is developed in MATLAB/Simulink environment which is designed to cope up with fluctuating input supply

voltages. The base signal for training and testing the neural controller, within this approach, is derived from the Simulink model which includes input supply voltages. This neural control system aims at regulating critical motor parameters such as speed and electromagnetic torque in real-time. Comparison results are made from neural network control obtained and the theoretically calculated values, confirming that it has efficiency. Thus, it demonstrates how neural networks are viable options in controlling BLDC motors under variable, unstable input voltages. These confirmations using MATLAB/Simulink are demonstrated for verification that the system works fast and does the intended action, verifying neural controllers for present-day motor control systems.

In [16], the research into the hybrid control scheme for controlling the speed of a BLDC motor finds it to be able to effectively deal with both reference current for the BLDC motor and DC bus voltage of the inverter, thus ensuring it is capable of better handling speed and performance for the motor. A Fractional Order Proportional-Integral-Derivative (FOPID) controller is utilized for the reference current of the motor in order to finely control the motor's speed. On the other hand, an FLC is employed for DC bus voltage adjustment of the inverter; it plays a significant role in providing a stable power supply with reduced ripples of voltage. Moreover, an advanced metaheuristic optimization technique in the form of the revised HS algorithm is implemented for the tuning of parameters for the FOPID controller. This optimization technique enhances system performance under changed operating conditions as in no loading, varying speeds, and other variable loads. The hybrid proposed controller is valid since it does ensure stable performances for the various motor conditions of operations.

Another further study reported in [17] also shows superiority by the use of the developed hybrid control configuration. Specifically, the system is exercised with three different states of the motor: no-load, variable load, and variable speed testing. This kind of testing confirms that the proposed hybrid control scheme is robust and versatile, especially considering real applications where the load and speed vary often. Precise speed control is ensured by the use of both FOPID and fuzzy logic controllers, while the Harmony Search algorithm effectively optimizes the control parameters, making the system adaptable and efficient. By integrating both continuous and discrete control techniques, the hybrid system provides superior regulation and responsiveness, ensuring minimal performance degradation under dynamic load and speed changes. The study shows that using multiple control strategies is an essential factor for the optimization of BLDC motor performance under various operating conditions, thus offering more efficient solutions as compared to other control methods.

The work reported in [18] deals with the design and implementation of an optimized FOPID controller through the HS metaheuristic algorithm, applied to speed control of a BLDC motor. A more flexible control method is introduced in the traditional PID framework by fractional orders in the FOPID controller, thereby allowing better tuning of motor speed under varying operational conditions. The HS algorithm is used to fine-tune the controller parameters so that the performance of the FOPID controller can be optimized. The system is tested under three different operating conditions: no load, varying loads, and varying speeds. This analysis proves the efficiency of the controller in its role of dealing with the intricacy of real dynamics of the motor. The findings show that the hybrid FOPID-Harmony Search approach can achieve better speed control with a higher degree of stability and responsiveness, thus composing an efficient solution for high-performance BLDC motor applications.

The paper in [19] presents a high-performance BLDC motor speed control scheme by an enhancement of a simple PID controller with fuzzy logic. In this design, although a traditional PID is used for effective performance in various applications, sometimes, because of the complexity and nonlinearity involved with motor dynamics or uncertainties in their operating conditions, PID controllers have proved inadequate. Using the PID with an incorporated fuzzy logic module can introduce better robustness and adaptability to conditions while allowing real-time feedback, allowing the motor to be at optimum performance, even with dynamically changing loads and changes in speed. The simulation results indicate a considerable improvement in the system performance. It reduces the transient time from 0.2 seconds to 0.05 seconds and eliminates overshoot, which is a common problem with conventional PID controllers. This study proves that the fuzzy-based PID controller improves the dynamics and stability of the BLDC motor, ensuring better response times and avoiding the risk of instability. Table 1 provides the summary points of the section.

Table 1: Summarization of the related works

Ref. No.	Techniques Used	Outcomes	Advantages	Disadvantages
[10]	Perturb and Observe (P&O)	Identifies maximum power point in PV systems	Simple and widely used MPPT method	Struggles under rapidly changing environmental conditions
[11]	Particle Swarm Optimization (PSO)	Optimizes MPPT for PV systems	Effective for optimization and real-time adjustments	Prone to premature convergence and local optima
[12]	Grey Wolf Optimizer (GWO)	Fast convergence to maximum power point for MPPT	Rapid adaptation to environmental changes	Performance degrades in complex, dynamic, or noisy environments
[13]	Artificial Bee Colony (ABC)	Efficient MPPT for unimodal objective functions	Low computational overhead and computational efficiency	Struggles with multi-modal and high-dimensional search spaces
[14]	Grasshopper Optimization Algorithm (GOA)	Effective for fast tracking of maximum power point in PV systems	Strong global explorer with fast convergence	Requires fine-tuning for optimal performance
[15]	Neural Network-based Controller	Real-time speed and torque regulation in BLDC motors under fluctuating input	Verifies efficiency and real-time performance	Performance might degrade under unstable conditions
[16]	Hybrid Control (FOPID, Fuzzy Logic, Harmony Search)	Simultaneous control of reference current and DC bus voltage in BLDC motor	Stable under varying motor conditions (load, speed, etc.)	Needs parameter tuning for optimal performance in dynamic scenarios
[17]	Hybrid Control (FOPID, Fuzzy Logic, Harmony Search)	Robust performance under varying loads, speeds, and no-load conditions	Superior adaptability and efficiency	Requires complex integration of multiple controllers
[18]	FOPID Controller with Harmony Search	Optimized speed control for BLDC motor under varying conditions	High stability and responsiveness	Complexity in controller tuning
[19]	Fuzzy-based PID	Improved motor speed control with real-time feedback	Reduced transient time, eliminates overshoot	Requires accurate tuning for optimal performance

3. PROPOSED METHODOLOGY: OPTIMAL UTILIZATION OF GRID CONNECTED MICROGRID SYSTEM

The framework of the suggested solution using the suggested methodology is shown in Figure 1. Renewable energies are made up of MG systems, including as photovoltaic and wind turbine systems, which also incorporate batteries. In this case, the renewableWind turbines and photovoltaic resources are examples of naturally occurring electrical energy resources that can only be supplied by the MG.In addition to collecting energy gathered from the PV and wind infrastructure, the constructed sections were connected by a DC bus

connection when the electricity was transferred from the AC-DC converter to the demand and the MG.In this case, the traditional MPPT device controller managed the whole thing conversion.The DC–DC converters is necessary for batteries in order to predict charging, manage the amount of impact from releasing, and guide the charge current supply.

3.1 Designing Grid-Connected Systems Mathematically

The best grid-connected MG systems utilisation depends on the cost of producing electricity and the price of authority purchased by consumers. The following is the mathematical explanation of the objective feature:

$$SBmax = \sum_{i=1}^{n} b_i\,(pd_i) - \sum_{j=1}^{m} c_j\,(pg_j) \quad (1)$$

Pi and net Pi, respectively, are used to indicate the computed and required true power for the PV bus I. Additionally, Qi, net Qi, and specific reactive energy are shown as calculated.

$$G(v,\varphi) = \begin{cases} p_i(v,\varphi) - p_i^{Net} \\ q_i(v,\varphi) - P_i^{Net} \\ p_m(v,\varphi) - P_m^{Net} \end{cases} \quad (2)$$

For the PV bus m, the computed and defined electrical energy is conveyed by Qi and net Qi. In many buses, the voltage intensity and phase angle are represented by the symbols (v,φ).

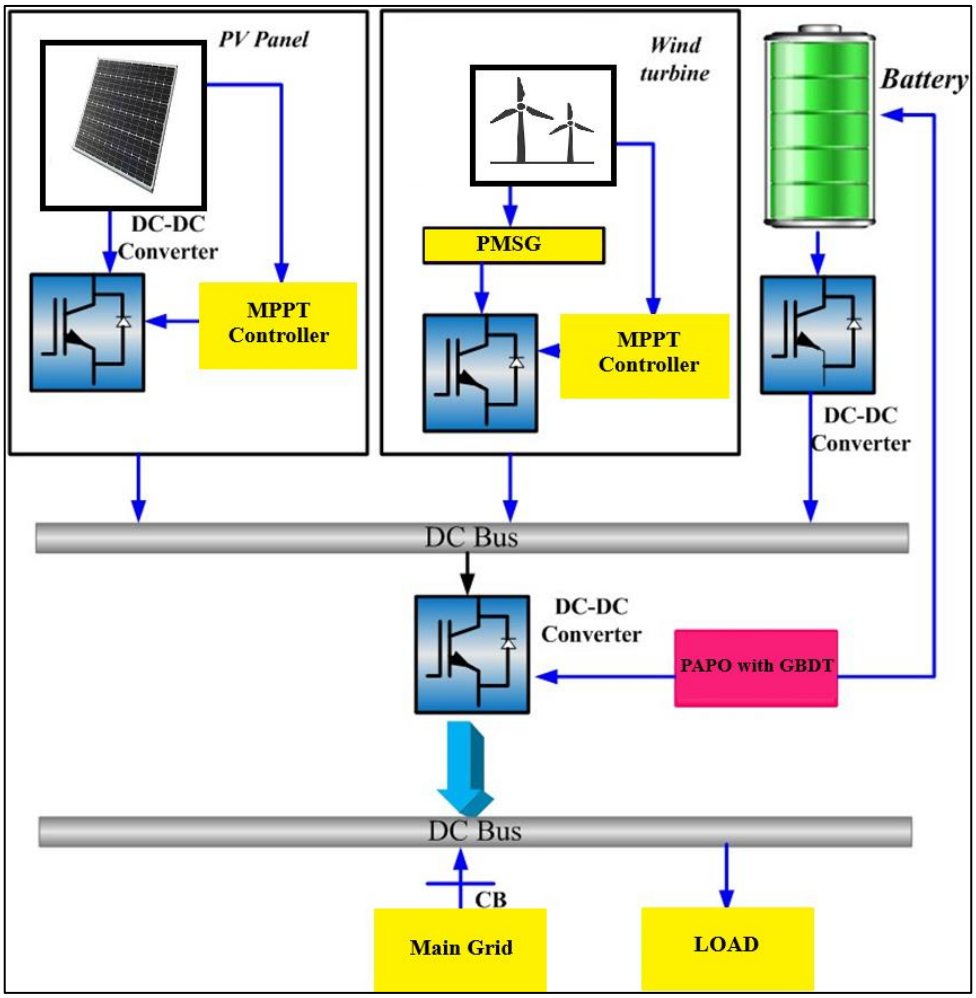

Figure 1: System design using the suggested methodology

3.2 Using an MG grid-connected system, an PAPO-GBDT-based controllers methodology achieves robust optimal utilisation.

Depending on the reliable optimum use of the grid-connected MG system, an effective optimization-based controllers approach with an embedded convert is described. Combining the PAPO and GBDT methods results in an effective optimization-based conversion approach. Using the recommended approach, PAPO conducts the evaluation process to set up appropriate control symbols for the network and builds an inventory of control indications for offline pathways based on the power type between the load side and supply side (batteries, electricity from renewable sources). The performed dataset fuels the GBDT technique for short implementation time and online control.

3.3 Optimisation Method For Priority Adaptive Particles (PAPO)

Optimisation of Fruit Fly The novel technique for identifying global optimisation in the fruit fly's food-finding behaviour is an algorithm. Compared to other organisms, fruit flies have greater senses and sensibility, especially in osphresis and eyesight. Fruit flies have superior eyesight and osphresis compared to other species. The fruit fly's osphresis organ were able to detect a wide variety of airborne odours, including food sources, up to 40 km away. Fruit flies may use their keen eyesight to locate food; if they are near, they may fly in that direction as well, and they may then locate the company's flocking site. Fruit specific order, and it communicates with other fruit flies to exchange information and compare the optimal spots for food searching. Fruit flies may determine fitness levels by taste; those with the highest fitness levels will fly in that direction. They fly in that direction and utilise their keen eyesight to locate food.The fly is an insect that may be found globally in both temperate and tropical climates.

The PAPO step-by-step process is as follows:

Step 1: Setup

Initialise the fruit fly's random fly direction and distance zone first, followed by the swarm's Location Range (LR), iteration count, and population size.

Step 2: The process of searching

Step 2.1: Each fruit fly is assigned an arbitrary path to find its distance to feed.

Step 2.2: The distance to the food source is used to calculate the starting position.

Step 2.3: The scent saturation judgement value is calculated.

Step 2.4: The scent strength of the distinct fruit fly site is calculated by feeding Si into the Smelli judgement mechanism.

Step 2.5: The maximum concentration of scent in fruit flies inside the swarm is determined by using the provided equation.

Step 3: The practice of vision hunting. The fruit fly swarming can fly in the direction of the setting, value of greatest focus, and coordinates of X and Y by employing vision.

Step 4: Optimisation via iteration

When the concentration of scent reaches the predetermined precision level, the iterative optimisation is initiated to repeat the execution of stages two through three.

3.4 GBDT processing

It combines a number of weak base algorithms for classification into one powerful model, usually a decision tree. ML techniques differ from classic boosting approaches owing to both favourable and adverse weight samples. The GBDT method converges globally using the zero-gradient orientation.

1: During the first step, the produced label is represented by Yi, and the starting continuous value of the model is expressed by the following equation.

$$f(X) = arg\min_{\beta} \sum_{j=1}^{n} I(y_i, \beta) \quad (3)$$

Step 2: The following formula is used to determine the gradients direction: In each residue,

The number repetition in the equation below is represented by the symbol m (m = 1).

$$Y_i - \left[\frac{\partial l(Y_i, f(X_i))}{\partial f(X_i)}\right]_{f(X)-f_m-1(x)} \quad (4)$$

Step 3: The initial framework is acquired and the information from the sampling is fitted utilising the fundamental classifier. The model's factor m a was determined, and the least squares method was used to fit the model.

$$a_m = arg\min_{\alpha,\beta} \sum_{i=1}^{N} [Y_i - \beta h(x_i, a)]^2 \quad [5]$$

Step 4: To minimise the loss function, the present modelling value is computed using the provided equation.

$$\beta_m = arg\min_{\alpha,\beta} \sum_{i=1}^{N} l(Y_i, f_{m-1}(X) + \beta h(x_i; a)) \quad (6)$$

Step 5: The updating the models process is stated at the supplied expression.

$$f_m(X) = f_{m-1}(X) + \beta_m h(x_i; a) \ (7)$$

Once the GBDT procedure is finished, the ideal controlling pulses is produced.

4. SIMULATION RESULTS AND INTERPRETATIONS

This section presents the grid-connected MG method's ideal use, which is implemented at the MATLAB/Simulink work site. In accordance with PAPO-GBDT management system efficiency, optimum utilisation is provided. Various case studies are taken into consideration in order to test and verify the efficacy of the proposed strategy. There are three different kinds of case studies used in the modelling section: (1) PV irradiation change under constant wind speeds (2) Wind speed fluctuates while PV irradiation remains constant. (3) There is a load problem when the PV's irradiation and wind speed are constant. The section below uses an illustration to show the exact demarcation of these three scenarios.

4.1 Example 1: PV Light Variation With Constant Breeze Velocity

Case 1 displays the The PV irradiance fluctuation with constant wind speed is seen in Figure 2. Subplot 2 (a) displays the amount of irradiance. The radiation level in this case is 1000 W/m2 at 0 seconds and stays there for 0.3 seconds. After then, it decreased to 500 W/m2, and around 0.55 to 0.65 seconds, it climbed to 800 W/m2. Then, at 0.68 to 0.9 seconds, it decreased to 400 W/m2. After that, the irradiance is raised to 700 W/m2 between 0.98 and 1 second. The wind speed is seen in Subplot 2 (b). In this case, the wind speed stays at 12 m/s. The efficiency evaluation of (a) PV and (b) current from batteries is shown in Figure 3. In subplot 3 (a), the PV current goes from 0 to 80 A in 0.01 seconds, stays steady for 0.3 seconds, and then drops to 40 A in 0.4 to 0.5 seconds. After then, the current is raised to 65 A in 0.5–0.7 seconds. After that, it decreased to 30 A in 0.8 to 0.9 seconds. Once again, the current is raised to 55 A in one second. The battery current is seen in Subplot 3 (b).

In this case, the battery's current increases from 0 to 280A in 0 seconds and then reaches its maximum of 330A. The power performance study using PV, wind, and batteries is shown in Figure 4. Solar energy is displayed in subplot 4 (a)flows between 0 and 3800W for 0.01 seconds. After then, it continues for 0.3 seconds. At 0.4 to 0.5 seconds, it decreased once again to 1500 W. After then, it rose to 2500 W and then, in 0.8 to 0.9 seconds, dropped to 1000 W. Subplot 4 (b) displays the wind power. Here, the wind power fluctuates between 0 and 2700W over a duration of 0 to 0.2 seconds, after which it stays steady for 0.3 to 1 seconds. Subplot 4 (c) displays the battery power.

In 0.01 seconds, the battery power increased from 0 to 4800 W, then in 0.3 seconds, it decreased to 4100 W. At 0.8 to 0.9 seconds, it then climbed to 5500 W. When one second passes, it hits 5000 W. The voltage performance analysis based on PV and batteries is shown in Figure 5. The PV voltage in subplot 5 (a) increased from 0 to 48V in 0.01 seconds, remained stable for 0.3 seconds, and then decreased to 32 A in 0.4 to 0.5 seconds. After then, the current is raised to 40 A in 0.5–0.7 seconds. After that, it decreased to 28 A in 0.8–0.9 seconds. Once again, the current is raised to 38 A in one second. The battery voltage analysis is shown in subplot 5 (b). In this case, the battery voltage dropped from 17.5 V to 16.79 V between 0 and 0.1 seconds. The load comparison between the suggested and current techniques is shown in Figure 6. In this case, the suggested PAPO-GBDT approach flows between 0 and 12000 4 W/10 W, and the mistake occurs at 1.22 between 0.6 and 0.7 seconds.

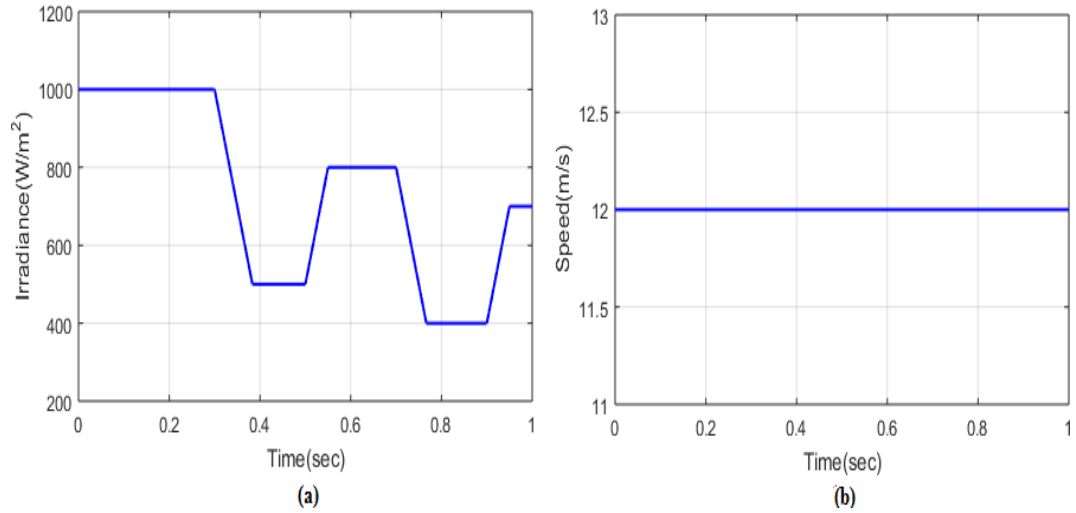

Figure 2: PV irradiance varies under constant wind speed (a) Irradiance (b) Wind speed

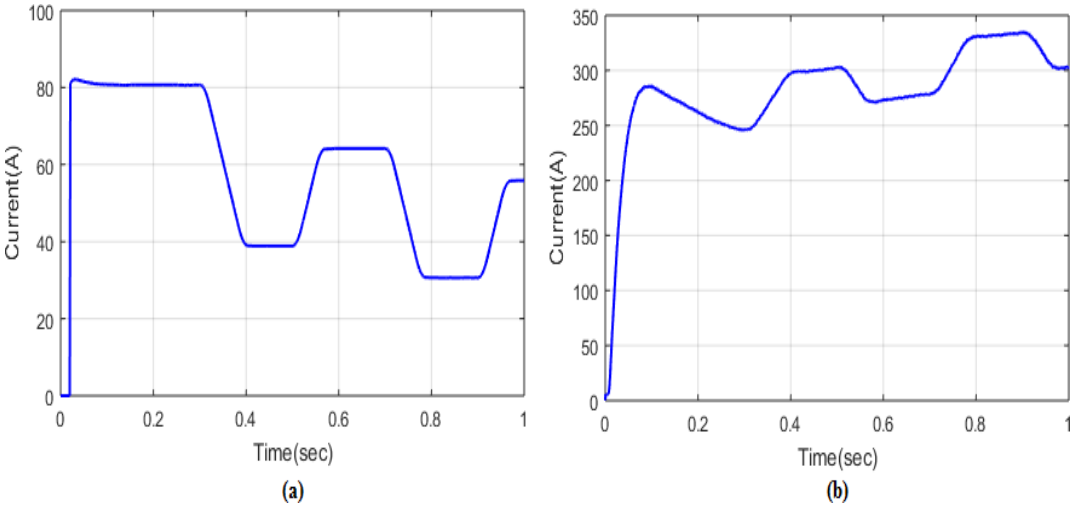

Figure 3: Performance analysis of current (a) PV (b) battery

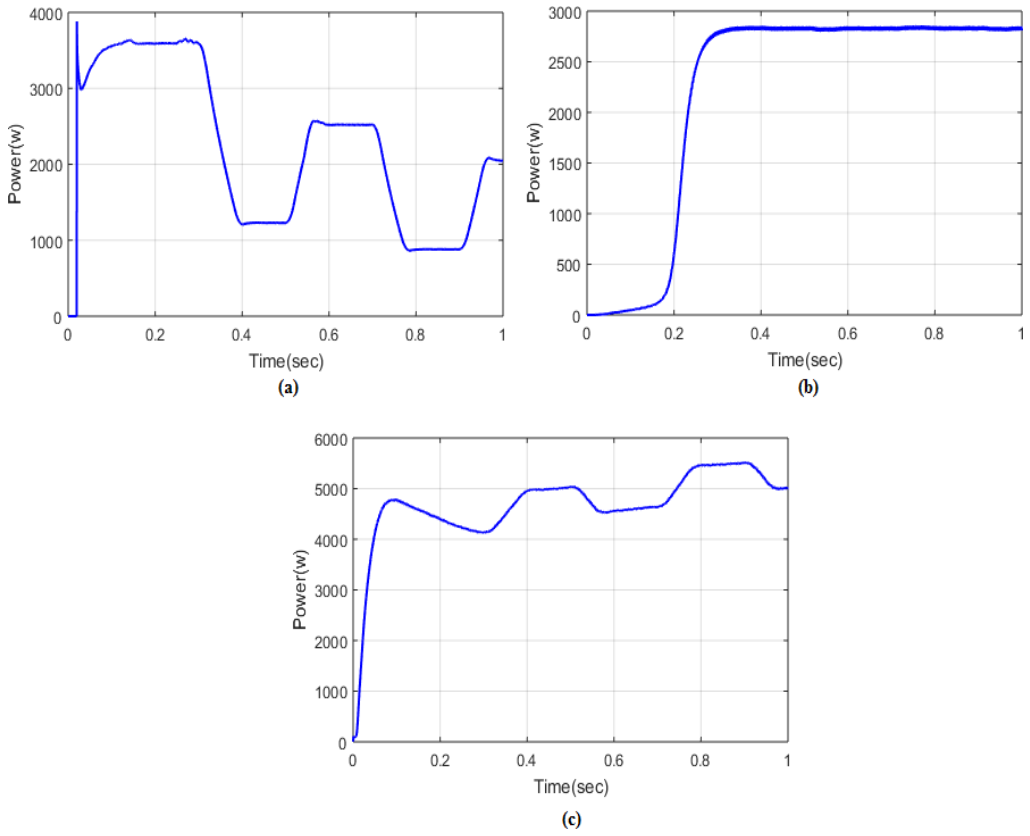

Figure 4: Performance analysis of power of (a) PV (b) wind (c) battery

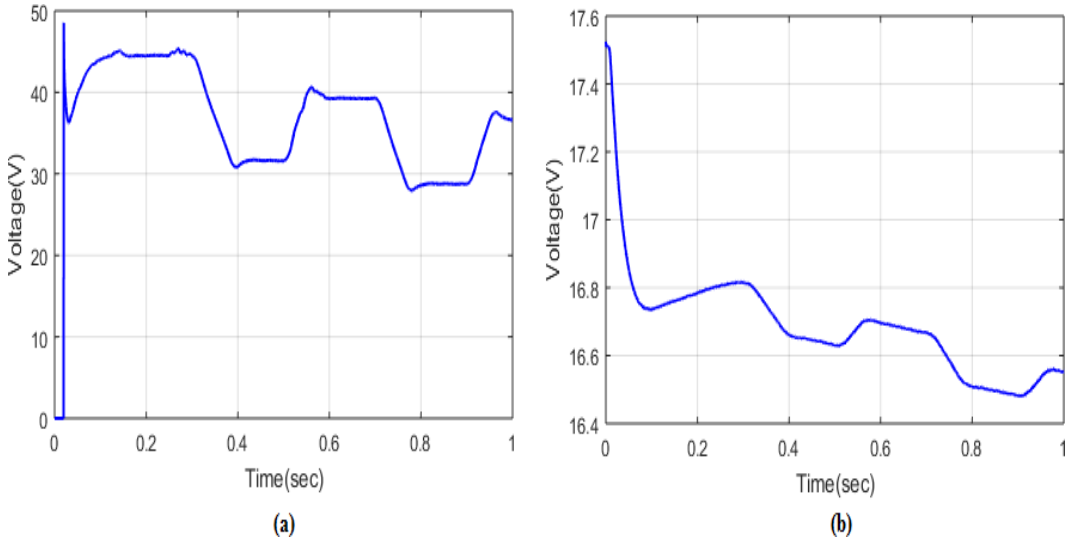

Figure 5: Performance analysis of voltage of (a) PV (b) battery

The connected mode produced the findings, which are seen in Figure 6. Hardware prevents a battery's state of charge from changing suddenly. As a result, both cases of demand dominant situation and renewable energy dominant situation each describe the full linked mode. In this case, each scenario runs for five minutes, for a total of ten minutes. As shown in Figure 6 (b) and (e), a battery's starting point of charge (SOC) is 81%, and both the irregular and direct current (DC) load is maintained at 502 watts during the process.

First scenario: The breeze emulation ran at 10 m/sec while the solar simulator ran at 710 w/m2 for 0–5 minutes. Currently, the RES produces 1040 watts of electricity, as seen in Figure 6 (c), with the solar generating 638 watts and the breeze from the wind turbines generating 416 watts. The extra power goes into the value system as seen in Figure 6 (a) because the produced RES power exceeds the load. A battery will use RES active power to charge if its state of charge (SOC) is lower than 90%. Figure 6 (e) displays the battery's matching recharging state of charge.

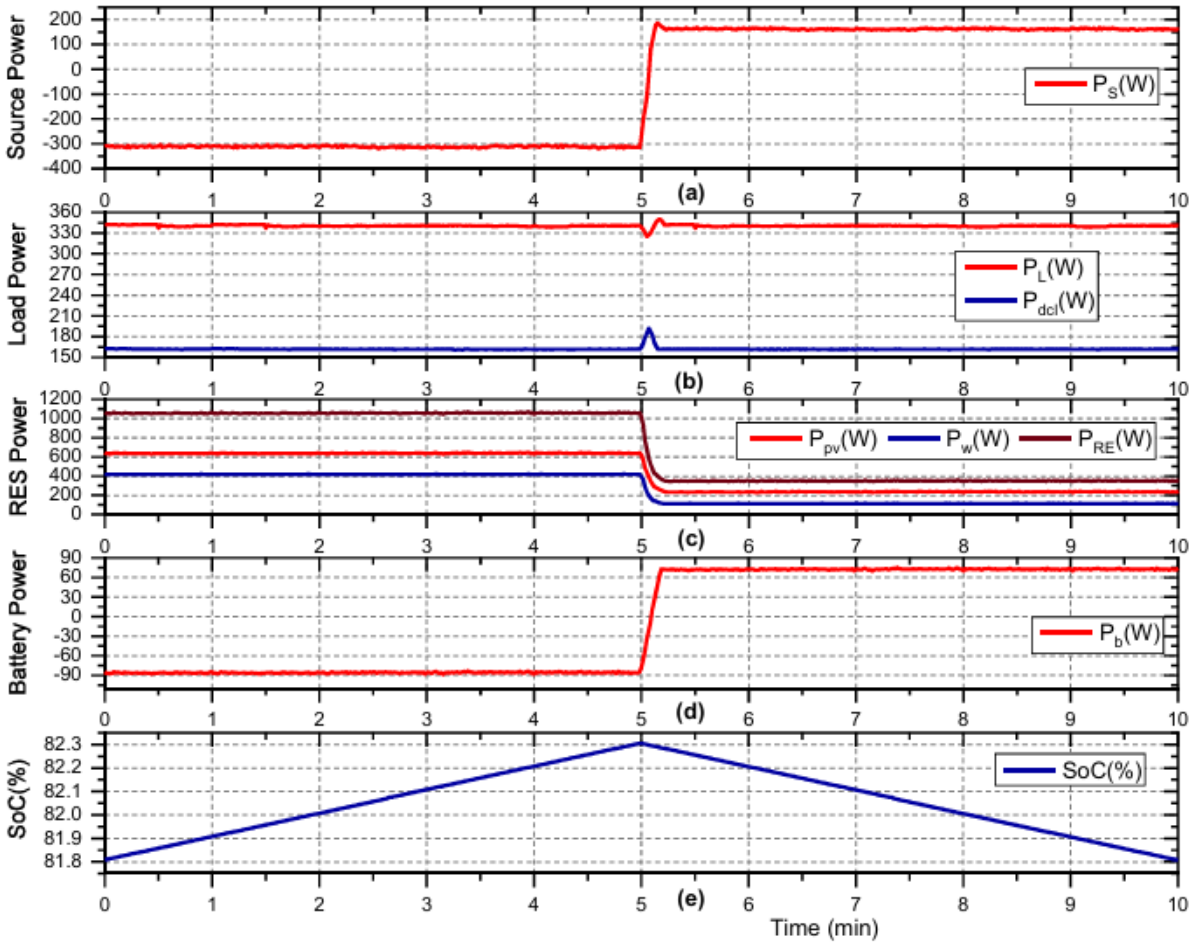

Figure 6: Connected style: PS (a), PL (b), PRE (c), Pb (d), and SoC

Case 2: The wind emulation ran at 6.8 m/sec while the solar simulation ran at 300 w/m2 for 5–10 minutes. As seen in Figure 6 (c), the total electricity produced by the RES is 350 watts under these conditions, with the solar generating 236 megawatts and the wind turbines generating 114 watts. As seen in Figure 6 (a-d), the utility grid and batteries provide the shortfall in electrical power since the produced RES energy is less than what is needed and the battery's state of charge (SOC) is more than 30%. As seen in Figure 6 (d), the battery will drain by supplying an active output of 72 watts when its state of charge (SOC) is higher than 30%. Figure 6 (e) displays the battery's equivalent discharging state of charge. Figure 6 illustrates how the power equilibrium among supplies and demands remains the same as a result.

Nevertheless, even when the power output in the DC connection fluctuates due to variations in solar and wind output, the voltage at the load is kept at the intended value (110V/ph) during this mode. In order to provide smooth power transmission between microgrid parts, the DC link voltage is also regulating more quickly, at around 281V. Additionally, the source current's THD is consistently less than 4%, and the supply side consistently maintains unity PF.

The issue occurs at 1.216 to 1.22W over 0.6 to 0.7sec in the current GA, ANFIS, AWO, and AWOA. The performance analysis of converter current in PV, wind, and battery is shown in Figure 7. The PV converter

current at subplot 7(a) increases from 0.01 to 118A for 0 seconds and then stays there for 0.3 seconds. At 0.4 to 0.5 seconds, it decreased once more to reach 50 A. After then, it rose to 90 A and then, in 0.8 to 0.9 seconds, dropped to 40 A. The wind current converter is shown in subplot 7(b). In this case, the wind current increases from 0 to 50 A in 0.01 seconds, then instantly decreases to 0 and changes again in 0.07 seconds, bPAPOre staying constant at 15 A in 0.25 to 1 seconds. The battery converter current is shown in subplot7(c). In this case, the battery current fluctuates between 0 and 280A between 0 and 0.1 seconds, and the modifications take place between 0.2 and 1 second.

Figure 8 shows the converter voltage performance evaluation in PV, wind, and battery. In subplot 8(a), the PV converters voltage fluctuates between 0 and 14V for 0 seconds, with the variations occurring between 0.4 and 0.8 seconds. The wind voltage converter is shown in subplot 8(b).

Here, the wind voltage fluctuates between 0 and 14V for a duration of 0 seconds, then stabilises between 0 and 0.2 seconds. The energy convert voltage is shown in subplot 8(c). In this case, the battery power fluctuates between 0 and 14V for 0.1 to 0.2 seconds, and the changes take place between 0.2 and 1 second.

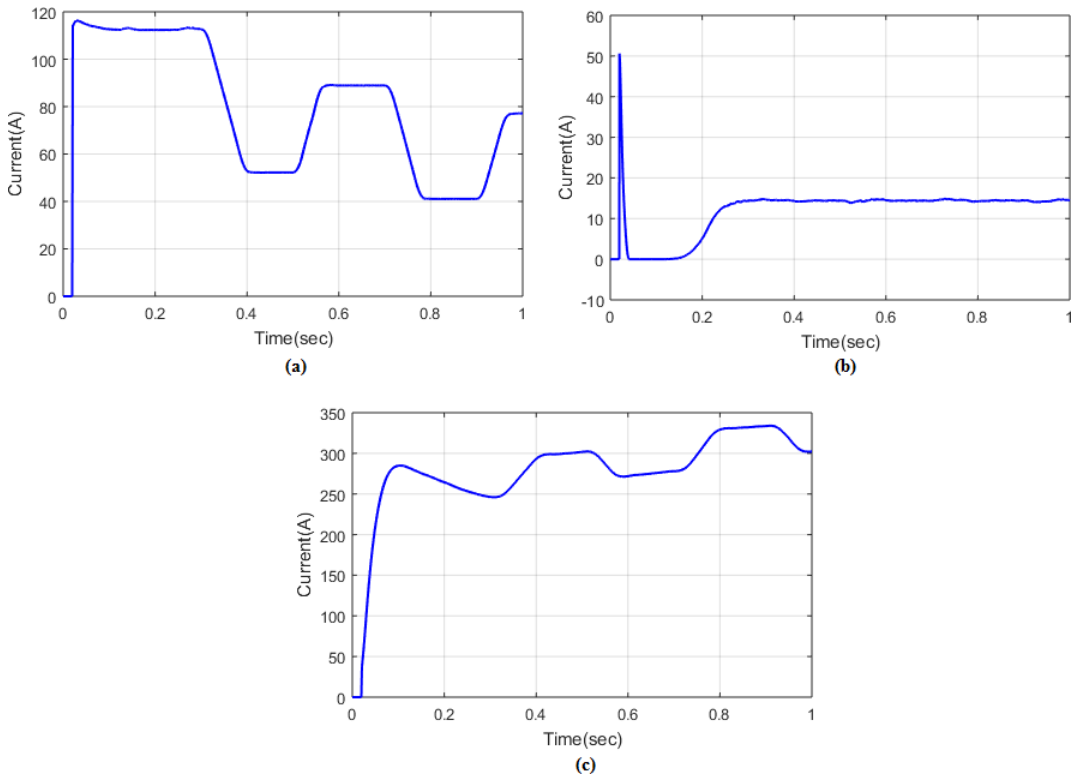

Figure 7: Performance analysis of current converter of (a) PV (b) Wind (c) battery

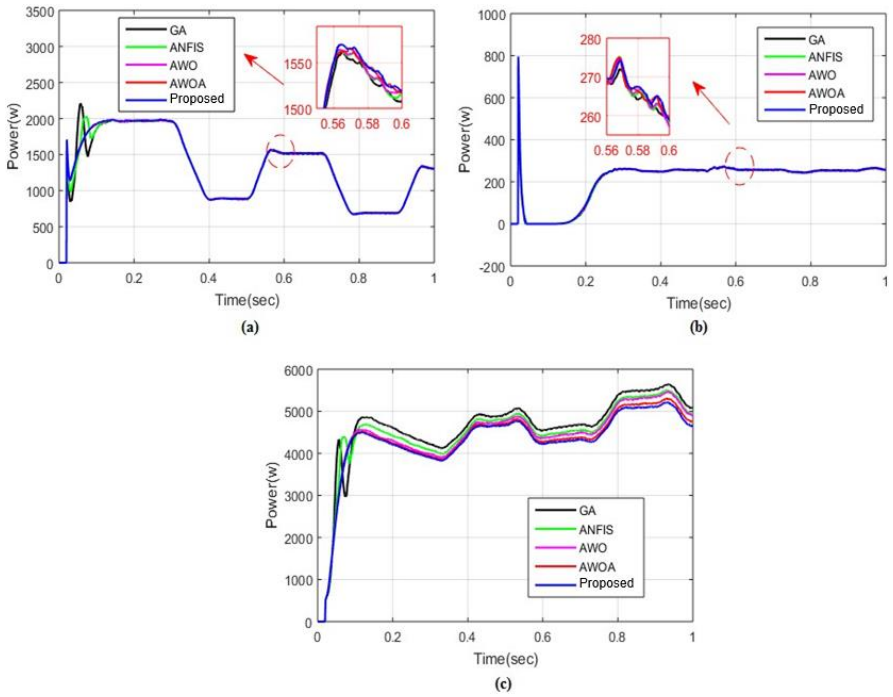

Figure 8: Unique power comparison of (a) PV (b) Wind (c) Battery

4.2 Example 2: Variability in Wind Speed Under Continuous PV The amount of sunlight

The load assessment between the suggested and current techniques is shown in Figure 9. In this case, the suggested PAPO-GBDT approach flows between 0 and 12000W, and the fault occurs at 1.222 between 0.55 and 0.65 seconds. The mistake occurs between 0.55 and 0.65 seconds at 1.224 to 1 in the current GA, ANFIS, AWO, and AWOA. The efficacy evaluation of converter current in PV, wind, and battery is shown in Figure 10. The PV converters current goes from 0 to 119A at axis 10(a) in 0 seconds and then stays constant until the conclusion of operating. A wind power exchanger is shown at subplot 10(b). Here, the wind's speed fluctuates between 0 and 50A for a duration of 0 seconds, and then between 0 and 0.2 and 1 seconds.

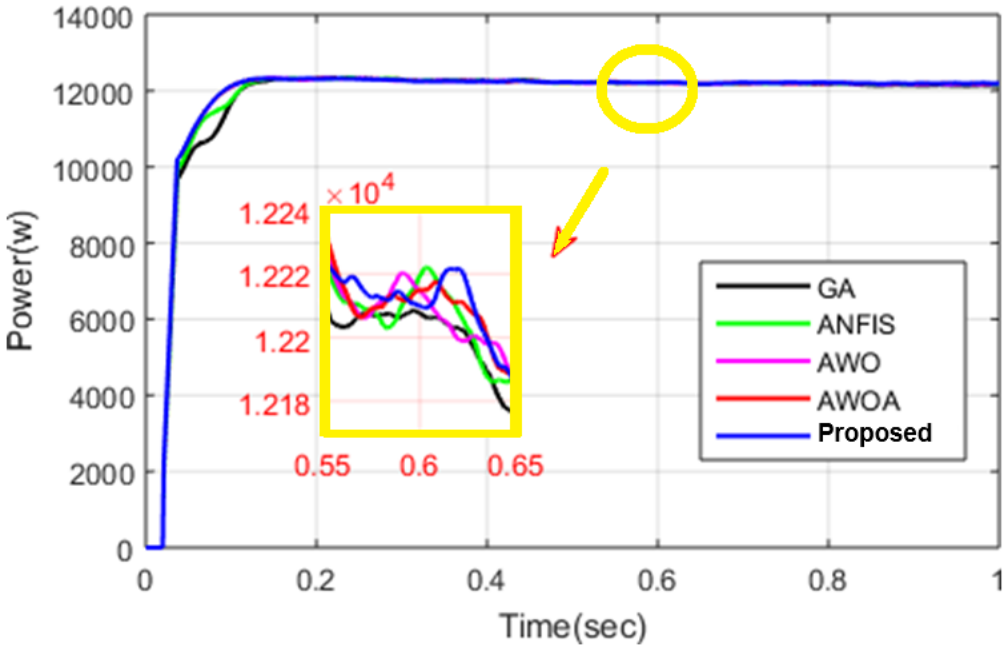

Figure 9: Individual Load comparison of proposed as well as existing methods

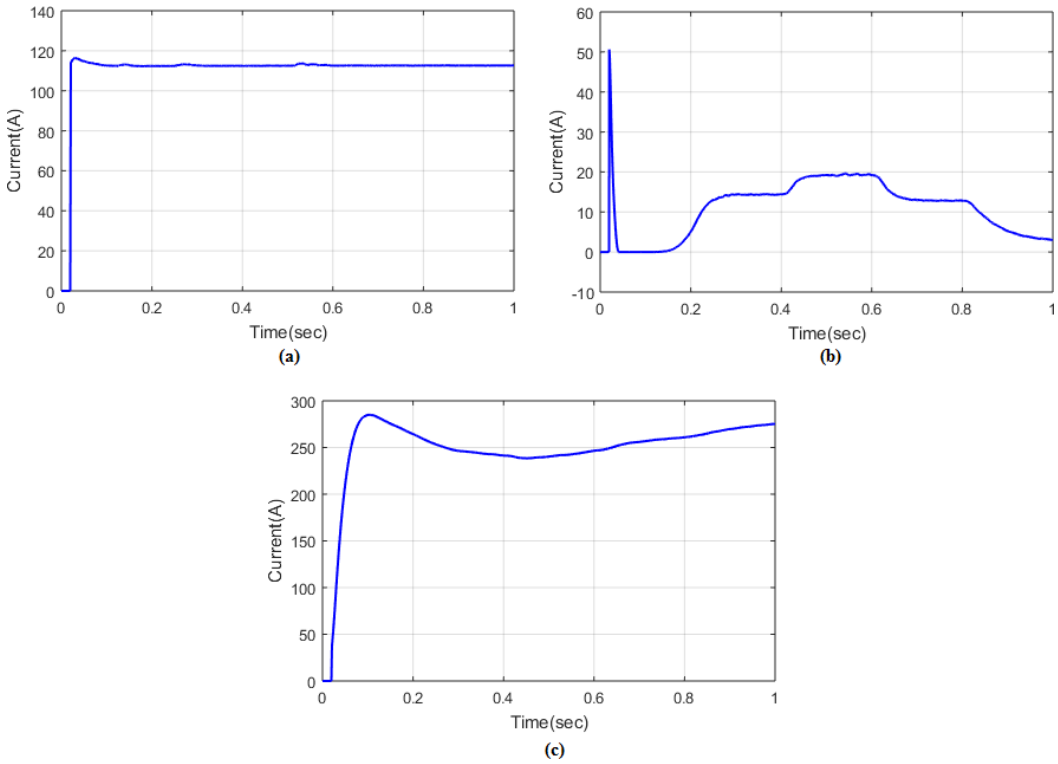

Figure 10: Performance analysis of current converter of (a) PV (b) Wind (c) battery

Table 2: System design using the suggested methodology

Control Parameters	GA	ANFIS	AWOA (1)	AWOA (2)	PAPO-GBDT
Active power controller					
G_{pp}	8.25	8.32	8.63	8.82	9.21
G_{pi}	0.20	0.30	1.65	1.86	1.90
Reactive power controller					
G_{qp}	5.09	5.36	7.69	8.17	8.36
G_{qi}	0.20	2.36	2.59	2.58	2.74

Table 3: The examination of statistical data is powered by 100 retries.

Solution Methods	C- 1 (Mean)	C- 1 (Median)	C- 1 (SD)	C-2 (Mean)	C- 2 (Median)	C- 2 (SD)
GA	0.897	0.885	0.025	0.868	0.872	0.007
ANFIS	0.884	0.881	0.028	0.867	0.845	0.005
AWO	0.837	0.863	0.031	0.866	0.855	0.005
AWOA	0.765	0.754	0.021	0.732	0.721	0.004
PAPO-GBDT	0.720	0.716	0.017	0.712	0.700	0.002

Table 4: Reactive energy statistics study with a hundred iterations

Solution Methods	C-1 (Mean)	C- 1 (Median)	C- 1 (SD)	C- 2 (Mean)	C- 2 (Median)	C- 2 (SD)
GA	0.932	0.915	0.023	0.946	0.927	0.006
ANFIS	0.901	0.918	0.028	0.976	0.934	0.007
AWO	0.823	0.822	0.024	0.856	0.835	0.003
AWOA	0.805	0.815	0.018	0.836	0.823	0.004
PAPO-GBDT	0.800	0.807	0.009	0.816	0.803	0.002

Table 5: Efficiency evaluation for two scenarios

Solution Methods	Case 1	Case 2
PAPO-GBDT	98.89	94
GA	87.76	84.76
ANFIS	87.76	84.76

The table 2 shows the comparison of different optimization techniques (GA, ANFIS, AWOA, PAPO-GBDT) for the control of active and reactive power. The parameters are Gpp, Gpi for the active power, and Gqp, Gqi for the reactive power, with the gains of each technique given for these controllers. The results reveal that PAPO-GBDT is superior to all other techniques with regard to both active and reactive power controller gains. For active power control, the maximum gain values achieved are with PAPO-GBDT at 9.21 for Gpp and 1.90 for Gpi. This shows superior performance in controlling the controller. In reactive power control, gains are again held by PAPO-GBDT at 8.36 for Gqp and 2.74 for Gqi, and this implies its approach to adjustment of power flow is better than others. Overall, this table shows that PAPO-GBDT performs the best for power controllers' optimization, and then GA and ANFIS methods are next with relatively good results but less gains.

Table 3 shows the statistical performance of various optimization techniques (GA, ANFIS, AWO, AWOA, PAPO-GBDT) with 100 iterations. Mean, median, and standard deviation (SD) values are reported for two cost functions, namely C-1 and C-2. In the case of C-1 (Mean), GA has outperformed other algorithms with a mean of 0.897, followed by ANFIS at 0.884, which shows better optimization. For C-1 (Median), GA also dominates the results and proves to be consistent in performance. AWOA and PAPO-GBDT have lower values, meaning that these methods are less stable or effective. For C-2 (Mean and Median), GA and ANFIS perform better than other methods, although PAPO-GBDT has better performance for C-2 SD with less variability. The results show that GA and ANFIS have more consistent and stable outcomes in general, while AWOA and PAPO-GBDT have relatively weaker performance metrics, especially consistency.

The table 4 compares the performances of different optimization techniques in reactive energy control for 100 iterations. It gives mean, median, and standard deviation statistics for the two cost functions, C-1 and C-2. GA stands out with high mean values both for C-1 and C-2 with the highest achieved by GA; C-1 Mean is 0.932 and C-2 Mean is 0.946, hence strong performance on both accuracy and energy control. The PAPO-GBDT method shows lower values, meaning it is not as effective in reactive energy optimization compared to GA and ANFIS. In terms of standard deviation, GA remains the most consistent method, having the lowest SD in both C-1 and C-2. AWO and AWOA perform relatively weaker, with their mean values being significantly lower, especially in the C-2 evaluation. This analysis shows that GA and ANFIS are more efficient than the others in reactive energy optimization. Table 5 Efficiency of optimization techniques for the two cases: Case 1 and Case 2 Efficiency values describe how well a method performs given the conditions. In this regard, PAPO-GBDT performs better with efficiency values of 98.89 for Case 1 and 94 for Case 2. This indicates that PAPO-GBDT has the best performance in both cases. On the other hand, GA and ANFIS achieve lower efficiencies, 87.76 and

84.76 for both cases, respectively, and hence are relatively weaker compared to PAPO-GBDT. However, GA and ANFIS still deliver respectable results. The lower efficiency values for AWO and AWOA further emphasize their comparative inefficiency. So, the results point out the optimization tasks at issue as the most effective approach since PAPO-GBDT excels under any complex or variable situation, whereas the other approaches, being effective, cannot be as good in terms of robustness over the experiments.

4.3 Evaluation of Performance

This section analyses the suggested approach's performance.The suggested system's performance is examined using established methodologies such as GA, ANFIS, and AWOA. Classes such asTP,TN,FP,FN are used to analyse the performance. Positive signals that are appropriately identified are TP. The negative signals that are appropriately identified are TN. Negative signals with incorrect labels are FP.

$$Acc = \frac{T_p + T_N}{T_P + T_N + F_P + F_N} \quad (8)$$

$$Precision = \frac{T_P}{F_P + T_P} \quad (9)$$

$$Spec = \frac{T_P}{F_N} T_P (10)$$

$$Sens = \frac{T_N}{F_P} T_N (11)$$

FN stands for incorrectly tagged positive signals. The equations are used to assess the performance.The efficacy compare between the suggested and current methods for 50 and 100 trials is shown in Table 6.

Table 6: A comparison of the suggested technique's effectiveness with the current approach for 50 and 100 trials

Metrics	50 Trials GA	50 Trials ANFIS	50 Trials AWOA	50 Trials Proposed	100 Trials GA	100 Trials ANFIS	100 Trials AWOA	100 Trials Proposed
Accuracy	0.86	0.78	0.92	0.96	0.90	0.75	0.89	0.96
Specificity	0.91	0.78	0.79	0.85	0.85	0.65	0.75	0.95
Recall	0.98	0.82	0.93	1.68	0.84	0.64	0.83	0.86
Precision	0.89	0.74	0.81	0.95	0.95	0.68	0.74	0.97

4.4 Evaluation of Modelling Metrics

This section evaluates the metrics based on MBE, MAPE and RMSE. The suggested system's overall efficiency is examined using the RMSE. If the MBE value is negative, the information is under-predicted. The correctness of the whole system is also calculated using the MAPE value. The following is how the metrics error is calculated:The RMSE, MAPE, and MBE of the suggested and current methods for 50 and 100 trials are shown in Table 7. At 50 trails, the suggested approach's RMSE, MAPE, and MBE values are 9.30, 0.93, and 0.98, respectively.

$$RMSE = \sqrt{\frac{\sum_{m=1}^{x}(n_o^k - n_t^k)}{x}} \quad (12)$$

$$MAPE = xa^* \sum_{m=1}^{z} \left| \frac{n_t^k - n_o^k}{n_t^k} \right| \quad (13)$$

$$MBE = x^* \sum_{m=1}^{x} n_t^k - n_o^k \quad (14)$$

At 100 trails, the suggested approach's RMSE, MAPE, and MBE values are 7.48, 1.95, and 2.78, respectively. At 50 trails, the AWOA approach's RMSE, MAPE, and MBE values are 22.4, 13.2, and 3.1, respectively. At 100 trails, the AWOA approach's RMSE, MAPE, and MBE values are 26.4, 14.8, and 7.9. At 50 trails, the ANFIS approach's RMSE, MPE, and MBE values are 15.9, 5.3, and 1.6, respectively. At 100 trails, the ANFIS approach's RMSE, MAPE, and MBE values drop to 23.1, 5.9, and 7.2, respectively. At 50 trails, the GA approach's RMSE, MAPE, and MBE values are 24.5, 16.8, and 6.1, respectively. At 100 trails, the GA approach's RMSE, MAPE, and MBE values are 27.9, 16.2, and 11.0, respectively.

Table 7: Comparing the suggested and current methods' modelling metrics for 50 and 100 tests

Metrics	**50trails**			
	GA	**ANFIS**	**AWOA**	**Proposed**
RMSE	24.5	15.9	22.4	9.30
MAPE	16.8	5.3	13.2	0.93
MBE	6.1	1.6	3.1	0.98
	100trails			
RMSE	27.9	23.1	26.4	7.48
MAPE	16.2	5.9	14.8	1.95
MBE	11.0	7.2	7.9	2.78

5.CONCLUSION

By using these two optimisation techniques separately, each of which has advantages and disadvantages of its own. Optimal controls are shown in terms of benefits, such as the ability to combine many cost functions, advance towards global optimum levels, and quick implementation, by using the PAPO optimiser independently. PAPO's disadvantages include the fact that each solution is solely dependent on the goal; people are free to pursue the local optimal of their own goals. Thus, the combination of GBDT and PAPO may accelerate global convergence and increase the technique's applicability to a variety of real-world scenarios. Consequently, an integrated approach is used in the study to circumvent the vulnerability brought about by the optimisation methodologies' individual application. TherPAPOre, a hybrid strategy yields superior results. Thus, it makes sense to use the PAPO-GBDT technique to implement the microgrid system that uses virtual inertia. The suggested method made use of the high performance converter architecture to improve converter efficiency, implement it effectively, regulate sources, and lower switching loss. Both the PAPO algorithm and the GBDT technique are used to optimise the gain parameter dataset and get the controller's ideal gain parameters. The suggested approach is implemented using the MATLAB/Simulink work site.

5. CONCLUSION

This paper introduced the Priority Adaptive Particle Optimization (PAPO) framework in combination with Gradient Boosting Decision Trees (GBDT) in order to optimize the control of bidirectional power converters and Brushless DC (BLDC) motors in microgrids. The approach managed to address problems associated with incorporating renewable energy sources, including solar and wind, into grid-connected microgrids in a sustainable manner that allows for efficiency in energy consumption. The system showed remarkable improvements in reducing power losses, improving energy conversion efficiency, and maintaining stable operation under changing environmental conditions through a series of case studies. The results of the

simulation studies in MATLAB/Simulink validate the effectiveness of the PAPO-GBDT approach in optimizing energy flow and managing load demand, outperforming conventional optimization methods. The adaptive control capabilities of the system allow for real-time adjustments in response to fluctuations in both energy generation and consumption, thus providing a reliable solution for dynamic microgrid operation. This work contributes to the development of more intelligent and robust energy networks to support growing demands for sustainable and efficient energy solutions. With the application of sophisticated optimization techniques, the framework is capable of accommodating diverse RESs, enhancing the scalability and cost-effectiveness of future smart grid system microgrid implementations.

REFERENCES

[1] Kumar, R. T., & Rajan, C. C. A. (2024). Optimized Hybrid Renewable Energy System for Sustainable Electric Vehicle Charging: Integration of Photovoltaic and Wind Power with Advanced Control Strategies. IEEE Access.

[2] Anbuchandran, S., Babu, M. A., Stephen, D. S., & Thinakaran, M. (2024). DC microgrid for EV charging station with EV control by using STSM controllers. Engineering Research Express, 6(4), 045345.

[3] Fouad, Z., Abd Elhak, B., Elhakim, D. A., & Abdelhalim, K. Energy Management Strategy with Regenerative-Breaking Recovery of Mixed Storage Systems for Electric Vehicles.

[4] Rihar, A., Nemec, M., Lavrič, H., Zajec, P., Vončina, D., Nedeljković, D., ... & Drobnič, K. (2024). Emerging Technologies for Advanced Power Electronics and Machine Design in Electric Drives. Applied Sciences, 14(24), 11559.

[5] Dayabhai, B. R. (2024). Power Management And Control For Microgrid (Doctoral Dissertation, Gujarat Technological University Ahmedabad).

[6] Gong, C., Li, Y. R., & Zargari, N. R. (2024). An Overview of Advancements in Multimotor Drives: Structural Diversity, Advanced Control, Specific Technical Challenges, and Solutions. Proceedings of the IEEE.

[7] Rao, S. N., Kumar, B. K., Suresh, Y. V., Kumar, A. S., & Manjunatha, B. M. (2024). Osprey optimization algorithm for MPPT of PV system with forward DC to DC converter under partial shading conditions. Engineering Research Express, 6(4), 045315.

[8] Itagi, A. R., Kallimani, R., Pai, K., Iyer, S., López, O. L., & Mutagekar, S. (2024). Cell Balancing Paradigms: Advanced Types, Algorithms, and Optimization Frameworks. arXiv preprint arXiv:2411.05478.

[9] Khallouf, K. N., Laid, Z., Benbouhenni, H., Debdouche, N., & Elbarbary, Z. M. S. Energy Reports.

[10] H. Abouadane, A. Fakkar, D. Sera, A. Lashab, S. Spataru, and T. Kerekes, ‘‘Multiple-power-sample based P&O MPPT for fast-changing irradiance conditions for a simple implementation,’’ IEEE J. Photovolt., vol. 10, no. 5, pp. 1481–1488, Sep. 2020.

[11] S. Obukhov, A. Ibrahim, A. A. Z. Diab, A. S. Al-Sumaiti, and R. Aboelsaud, ‘‘Optimal performance of dynamic particle swarm optimization based maximum power trackers for stand-alone PV system under partial shading conditions,’’ IEEE Access, vol. 8, pp. 20770–20785, 2020.

[12] A. D. G. Jegha, M. S. P. Subathra, N. M. Kumar, U. Subramaniam, and S. Padmanaban, ‘‘A high gain DC–DC converter with grey wolf optimizer based MPPT algorithm for PV fed BLDC motor drive,’’ Appl. Sci., vol. 10, no. 8, p. 2797, Apr. 2020.

[13] S. Motahhir, A. Chouder, A. E. Hammoumi, A. S. Benyoucef, A. E. Ghzizal, S. Kichou, K. Kara, P. Sanjeevikumar, and S. Silvestre, ‘‘Optimal energy harvesting from a multistrings PV generator based on artificial bee colony algorithm,’’ IEEE Syst. J., vol. 15, no. 3, pp. 4137–4144, Sep. 2021.

[14] M. Chankaya, I. Hussain, A. Ahmad, H. Malik, and F. P. G. Márquez, ‘‘Multi-objective grasshopper optimization based MPPT and VSC control of grid-tied PV-battery system,’’ Electronics, vol. 10, no. 22, p. 2770, Nov. 2021.

[15] I. Saleh, A. A. Bature, S. Buyamin, and M. A. Shamsudin, ‘‘Speed control of a BLDC motor using artificial neural network with ESP32 microcontroller based implementation,’’ in Control, Instrumentation and Mechatronics: Theory and Practice. Cham, Switzerland: Springer, 2022, pp. 358–368.

[16] P. Saravanan, R. G. Raj, P. Sekhar, and P. Vijayarajan, ‘‘Speed control of brushless DC electric motor (BLDC) motor using hybrid Takagi Sugeno fuzzy logic and enhanced gravitational search algorithm with PSO,’’ Electr. Power Compon. Syst., vol. 52, no. 9, pp. 1692–1705, May 2024.

[17] S. Pandeeswari and S. Jaganathan, ‘‘Dual stage speed control of BLDC motor using hybrid QPSO-CSO technique,’’ Electr. Power Compon. Syst., vol. 52, no. 1, pp. 67–81, Jan. 2024.

[18] M. A. M. Eltoum, A. Hussein, and M. A. Abido, ‘‘Hybrid fuzzy fractional order PID-based speed control for brushless DC motor,’’ Arabian J. Sci.Eng., vol. 46, no. 10, pp. 9423–9435, Oct. 2021.

[19] M. Sundaram, J. Chelladurai, M. Anand, M. S. S. Kumari, S. Sharma, and M. E. H. Assad, ‘‘A novel approach to energy-optimized variable-speed sensorless-based brushless DC motors (BLDC) control for automotive wiper applications,’’ Arabian J. Sci. Eng., vol. 49, no. 2, pp. 1491–1504, Feb. 2024.

[20] Sadeghi, A., Bellavista, P., Song, W., & Yazdani-Asrami, M. (2024). Digital Twins for Condition and Fleet Monitoring of Aircraft: Towards More-Intelligent Electrified Aviation Systems. IEEE Access.

[21] Chu, Y., & Hu, F. (2024). Presenting a new method for optimal placement of reliability-based distributed generation units in the transmission system considering the demand response schedule. Electrical Engineering, 1-15.

[22] Mokhlis, H., & Siano, P. (2024). Eighth International Conference on Energy System, Electricity, and Power (ESEP 2023). In Proc. of SPIE Vol (Vol. 13159, pp. 1315901-1).

[23] Takialddin, A. S., Al-Salmany, Z. T., Al-qawasmi, K., Al Mashhadany, Y., Algburi, S., Mohammed, O. H., & Al-Smadi, A. High-Performance Simulation and Analysis of Hybrid Renewable Energy On-Grid Systems. Available at SSRN 5018868.

[24] Dognini, A. Multi-criteria service restoration methods for AC and AC/DC distribution grids (Doctoral dissertation, Dissertation, RWTH Aachen University, 2024).

[25] Naik, S. C., AH, M. H. A., Lobo, A. R., Sona, S. S., & Badiger, M. (2024). A Comprehensive Review of Electric Vehicles. E-Mobility in Electrical Energy Systems for Sustainability, 257.